Journal of Physics: Conference Series **653** (2015) 012162 doi:10.1088/1742-6596/653/1/012162

The study of ionization by electron impact of a substance simulating spent nuclear fuel components

N N Antonov, E I Bochkarev, A V Gavrikov, A A Samokhin and V P Smirnov

Joint Institute for High Temperatures of the Russian Academy of Sciences, Izhorskaya 13 Bldg 2, Moscow 125412, Russia

E-mail: antonovnickola@gmail.com

Abstract. Plasma sources of model substances are necessary to solve problems associated with development of the spent nuclear fuel (SNF) plasma separation method. Lead was chosen to simulate kinetic and dynamic properties of the heavy SNF components. In this paper we present the results of a study of a lead vapor discharge with a lead concentration of 10^{12}–10^{13} cm^{-3}. Ionization was carried out by an electron beam (with energy of up to 500 eV per electron) inside a centimeter gap between planar electrodes. The discharge was numerically modeled using the hydrodynamic and single-particle approximation. Current–voltage characteristics and single ionization efficiency were obtained as functions of the vapors concentration and thermoelectric current. An ion current of hundreds of microamperes at the ionization efficiency near tenths of a percent was experimentally obtained. These results are in good agreement with our model.

1. Introduction

One of the priorities of nuclear power industry is the reprocessing of spent nuclear fuel (SNF). The possibility of using plasma separation method as a basis of the reprocessing technology of SNF is widely discussed nowadays [1–5].

One needs a plasma sources of model substances to simulate experimentally the plasma separation method. A productivity near 100 microamperes is sufficient for the pilot experiments. In this article we present some results of development of a lead electron-beam plasma source. Lead simulates kinetic and dynamic properties of heavy components of a spent nuclear fuel. It is worth noting that for industrial realization of this method the plasma source productivity near 1000 gr/hr is required. A source of this kind can be based on vacuum arc discharge [6].

2. Model

We carry out a simulation of the electron-beam discharge in the lead vapor of concentration of $10^{12} \ldots 10^{13}$ cm $^{-3}$ in the gap between flat electrodes. One of the electrodes was a hot cathode. The distance between the electrodes $d = 1$ cm, the potential difference was up to 500 V. The lead vapor was injected into the interelectrode space with an energy $\varepsilon_a \sim 0.1$ eV.

Consider the case in which an influence of produced ions can be neglected. The dependence of potential φ on coordinate x in the interelectrode space is basically determined by the Child–


Content from this work may be used under the terms of the Creative Commons Attribution 3.0 licence. Any further distribution of this work must maintain attribution to the author(s) and the title of the work, journal citation and DOI.
Published under licence by IOP Publishing Ltd

Langmuir law:

$$\varphi = \left(\frac{9\pi\sqrt{m}}{\sqrt{2e}}J_e\right)^{2/3} x^{4/3},$$

where e is electron charge and m is electron mass.

The electric field $E(U,\varphi)$ in the interelectrode space can be written as

$$E(U,\varphi) = 4/3\frac{U^{3/4}\varphi^{1/4}}{d},$$

where U is a potential difference between the electrodes. The density J_i of ion current may be written as

$$J_i = n_a V_i J_e, \tag{1}$$

where n_a is a concentration of lead atoms in the ionization region.

$$V_i(U) = \int_0^U \frac{\sigma_i(\varphi)}{E(U,\varphi)}d\varphi,$$

where $\sigma_i(\varphi)$ is the ionization cross section of lead atoms [7].

Ionization efficiency η is the ratio of ion flux to the flux of atoms. η does not depend on the vapor density n_a in the interelectrode space:

$$\eta = \frac{V_i J_e}{e v_a} = 0.78 \times 10^{13}\sqrt{\frac{A}{T_a}}V_i J_e,$$

where v_a is a velocity (cm/s) of lead atoms, T_a is the lead vapor temperature (eV), A is the lead atomic weight (207.2). For lead atoms with the vapor temperature $T_a = 0.1$ eV, $J_e = 5$ mA, and $V_i = 5 \times 10^{-16}$ cm^3 the ionization efficiency η is $0.9 \times 10^3(0.09\%)$.

Consider the case in which the influence of the produced ions is significant. The increase of the lead density up to 6×10^{12} cm^{-3} results in equalizing the ion density n_i and electron density n_e. This has a significant impact on the potential distribution in the interelectrode space.

Assuming that $J_i \ll J_e (J_e = const)$ in the whole interelectrode space and taking into account the resonant charge exchange, one can write the spectral density of the ions $f_i(\varphi,\varepsilon)$ (A/(cm$^2\times$eV)), the concentration of singly ionized ions n_i and the current density J_i as:

$$-\frac{dJ_i}{dx} = n_a\sigma_{+1}(\varphi)J_e, \tag{2}$$

$$f_i(\varphi,\varepsilon) = -\frac{1}{E(x')}\frac{d}{dx'}[e^{n_a\sigma_{exch}(x-x')}J_i(x')], \tag{3}$$

$$\varphi(x') = \varphi(x) + (\varepsilon - \varepsilon_a), \tag{4}$$

$$n_i(x) = -4.5 \times 10^{12}\sqrt{A}\int_x^d \frac{d}{dx'}\left(e^{n_a\sigma_{exch}(x-x')}J_i(x')\right)\frac{dx'}{\sqrt{(\varphi(x') - \varphi(x)) + \varepsilon_a}}, \tag{5}$$

where ε is the ion energy at coordinate x with potential $\varphi(x)$, σ_{+1} is the ionization cross section of a singly ionized lead atom. A dependence of resonant charge exchange cross section on energy was not considered in the calculations. Its value was taken equal to $\sigma_{exch} = 80\times10^{-16}$ cm^2 [8]. An influence of doubly ionized ions was not considered in the model because of a small probability of

their production. If we take into account a spectral density of the ions $f_i(\varphi, \varepsilon)$ then the equation for the potential becomes:

$$\frac{d^2\varphi}{dx^2} = \beta J_e \left(\sqrt{\frac{m_e}{m_i}} \frac{1}{\sqrt{\varphi}} - \int_x^d e^{n_a \sigma_{exch}(x-x')} \frac{\sigma_{+1}(\varphi(x')) + n_a \sigma_{exch} V_i(x')}{\sqrt{(\varphi(x') - \varphi(x)) + \varepsilon_a}} n_a dx' \right), \qquad (6)$$

$$\beta = 4\pi \times 9 \times 10^{11} \sqrt{\frac{m_i}{2k_B}} = 0.81 \times 10^7 \sqrt{A} \left(\frac{V \times eV^{1/2}}{A} \right),$$

where k_B is the Boltzmann constant (erg/eV).

Diagrams in figure 1 show the ion current density (J_i) versus voltage at several values of thermoelectron current at the concentration n_a of 1×10^{12} cm^{-3} and 2×10^{12} cm^{-3}.

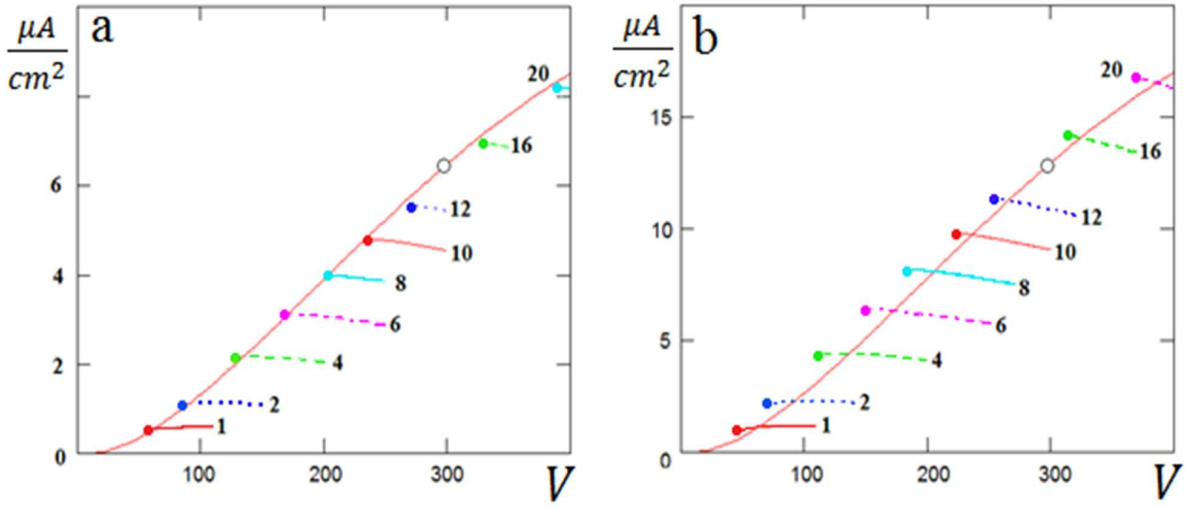

Figure 1. The ion current density CVC. Thermoelectron current $J_e = 1$, 2, 4, 6, 8, 10, 12, 16, 20 mA/cm^2. (a) $n_a = 1 \times 10^{12}$ cm^{-3} (b) $n_a = 2 \times 10^{12}$ cm^{-3}. Solid line ○ is equation (1).

Figure 1a shows that the numerical value of the current–voltage characteristics (CVC) extreme points obtained by solving the equations (2,5,6) are in a good agreement with the numerical values obtained by solving the equation (1). When the concentration n_a of lead atoms increases, the ion influence becomes more significant and a difference between the numerical values of the CVC extreme points and the numerical values obtained by solving the equation (1) increases (see figure1*b*).

Analysis of ion current density CVC shows that when the lead vapor density n_a approaches 6×10^{12} cm^{-3} the ion ● ($n_e < n_i; E_{(x=d)} = E_A = 0$) and the electron ○ ($n_e > n_i; E_{(x=0)} = E_K = 0$) branches can be realized depending on the magnitude of the electron current and the potential (see figure 2). E_K is the electric field intensity at the electron emitter. E_A is the electric field intensity at the electron collector.

Figure 2 shows that the ion branch regime is realized at lower currents ($J_e < 45$ mA/cm^2) and voltages ($U < 250$) than the electron branch regime. The x-distribution of electric field intensity is shown in the figure 3. Figure 3a shows the case of approaching the ion branch along the CVC, which corresponds to $J_e = 30$ mA/cm^2. Figure 3b shows the case of approaching the electron branch along the CVC, which corresponds to $J_e = 50$ mA/cm^2.

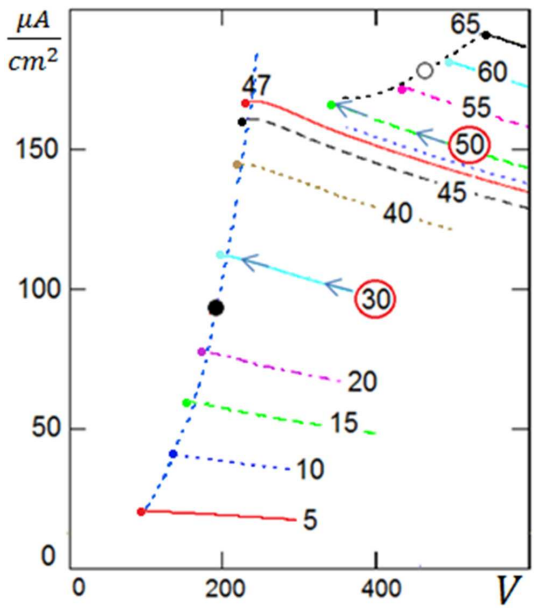

Figure 2. The ion current density CVC. $n_a = 6 \times 10^{12}$ cm^{-3}. Ion branch ● (J_e = 5, 10, 15, 20, 30, 40, 45 mA/cm^2). Electron branch ○ (J_e = 47, 48, 50, 55, 60, 65 mA/cm^2).

Figure 3a shows that in the ion branch regime the electric field intensity depends on x almost linearly everywhere in the interelectrode space. This allows one to construct a simplified theory for the case when $n_e < n_i$, $E_{(x=d)} = E = 0$. Curve ● (see figure 2) was obtained by solving Poisson's equation with a linear electric field intensity dependence in the interelectrode space. Figure 2 shows that the numerical value of the CVC extreme points obtained by solving the equations (2,5,6) are in a good agreement with the numerical values of ● curve. The electron

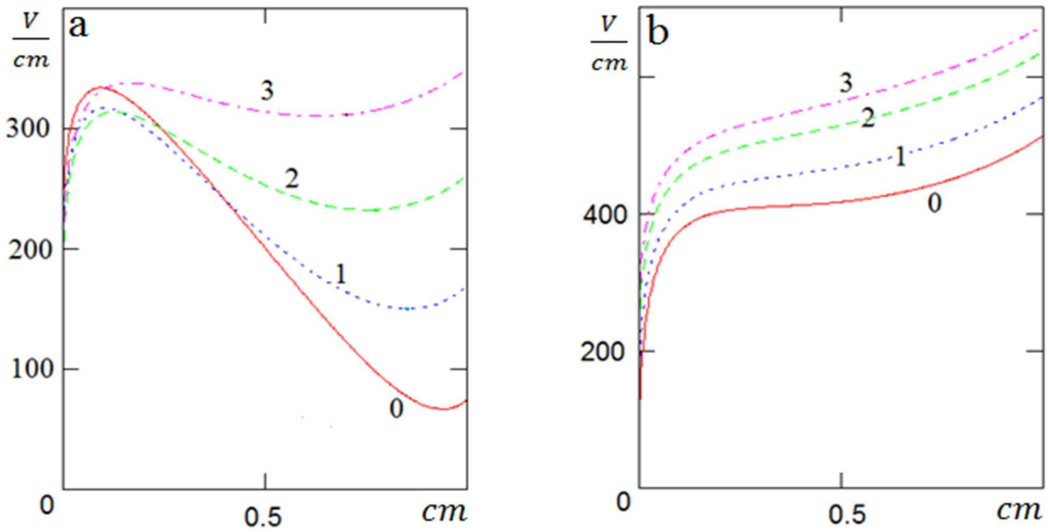

Figure 3. The electric field intensity versus x-coordinate. (a) Ion branch J_e = 30 (mA/cm^2) U = 200 V (curve 0), 222 V (curve 1), 265 V (curve 2), 322 V (curve 3). (b) Electron branch J_e = 50 mA/cm^2) U = 420 V (curve 0), 468 V (curve 1), 527 V (curve 2), 563 V (curve 3).

branch of CVC curve ○ (see figure 2) was constructed from the extreme points of the I–V curve which was derived from the equations (2,5,6). The numerical simulation reveals that the ionization efficiency at the concentration $n_a = 8{\times}10^{12}$ cm^{-3} is twice of that at $n_a = 6{\times}10^{12}$ cm^{-3} and reaches 0.8% ($\eta = 8 \times 10^{-3}$).

3. Experiment

The experimental module consists of two main parts: the evaporator cell and the ionization unit. Evaporation of the model substance was carried out by a crucible heating. The material flow injecting into the ionization area was formed by a hole of 1 mm in diameter. The heating was carried out by a tungsten filament of 0.3 mm in diameter. The maximum heater power is 100 watts and the maximum temperature inside the evaporator cell is 1450 K. Ionization unit is a system consisted of three electrodes (electron emitter, electrons collector, and ion collector). It is worth noting that in the considered calculation model the system consists of two plane electrodes but in the experiment an ion collector was added to them. This collector is necessary for measuring the number of ions produced in the discharge region. The experimental setup is shown in figure 4. In our experiments the potential difference between the ion collector and the electrons emitter U_i did not exceed 150 V and between the electrons collector and electrons emitter U_e it did not exceed 500 V. The electron emitter was realized as a system of two parallel tungsten filaments (of 200 microns in diameter) and a flat stainless steel plate.

The distance from the evaporator hole to the ionization region is 1.5 cm. The distance from the thermionic filaments to the diagnostic ion collector is 0.5 cm. Air was used as a buffer gas. Its residual pressure does not exceed 1×10^{-4} Torr. It is worth noting that the realized system is close to the ion source proposed and developed by Freeman in 1963 [9].

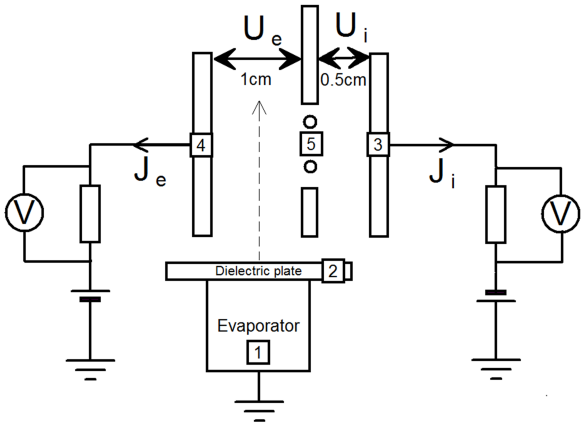

Figure 4. Experimental setup: 1—evaporator, 2—dielectric plate, 3—collector of ions, 4—collector of electrons, 5—hot cathode.

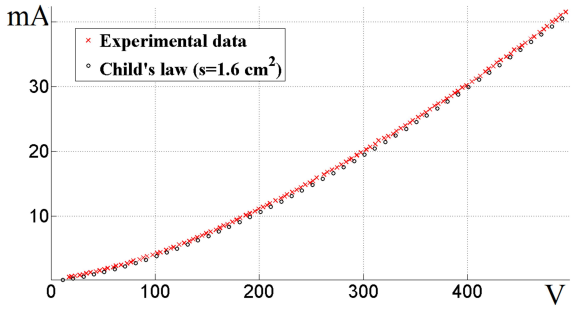

Figure 5. The diode I–V curve at potential difference $U_i = -50$ V.

In the initial stage of the experiment the potentials of electrodes (U_e and U_i) and the parameters of the hot cathode filament (thermoemission current) were held constant. After that the measurement of the diode I–V curve were done. Next lead was heated in the evaporation cell. During the experiment the evaporation cell temperature and the currents J_i and J_e were measured. Evaluations of matter flow and concentration were based on the measurement of evaporation cell temperature.

The diode I–V curve is shown in figure 5. The working electrode area was $s = 1.6$ cm^2.

Figure 6 shows the results of the experiment with $U_e = 350$ V and $U_i = -50$ V. The temperature inside the evaporator cells increased from 300 K to 1450 K.

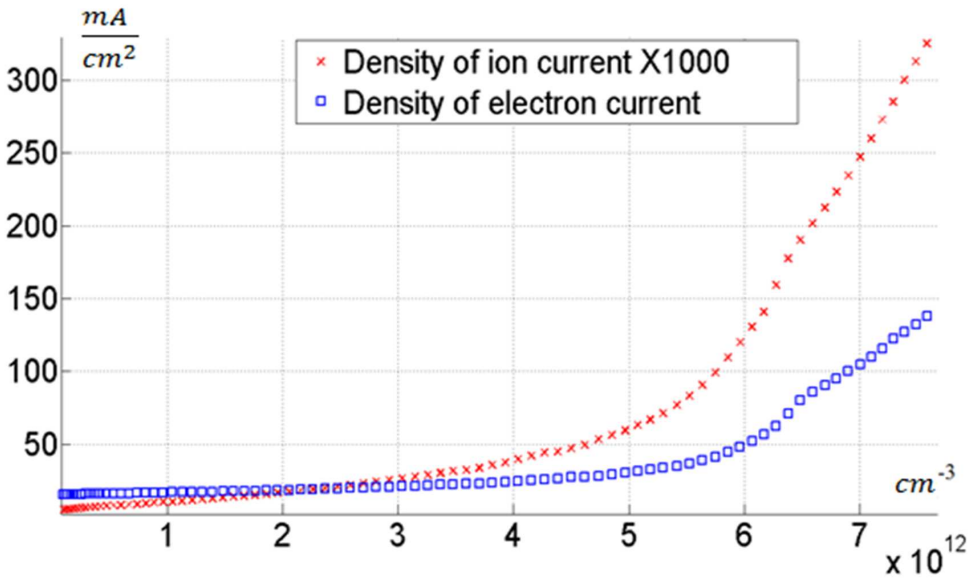

Figure 6. Dependence of the ion J_i and electron current J_e density on concentration n_a of lead vapors in the ionization region ($U_e = 350$ V and $U_i = 50$ V). The ion current scale is magnified by a factor of 1000.

Table 1 compares the experimental results (see figure 6) and the results of simulation (see figure 1 and figure 2).

Table 1. Comparison of calculated and experimental data.

n_a, cm^{-3}	J_e, mA/cm^2	J_i (Model), μA/cm^2	J_i (Experiment), μA/cm^2
1×10^{12}	16	7	10
2×10^{12}	18	16	17
6×10^{12}	50	150	130

It can be seen that the experimental and theoretical results are in a good agreement. The experimental value of ionization efficiency at a concentration of 6×10^{12} cm^{-3}(with the potential difference $U_e = 350$ V and electron current $J_e \approx 50$ mA/cm^2) reached 0.26%.

4. Conclusion

Experimental results are in a good agreement with the computational model. The discharge in the lead vapor with a density from $n_a = 10^{12}$ to $n_a = 10^{13}$ cm^{-3} was studied. CVC and single ionization efficiency were obtained as a function of vapor concentration and thermoelectron current both in the computational model and experimentally. The maximum ionization efficiency that obtained by the modeling is near 0.8%. The lead ion current density up to 300 μA/cm^2 was experimentally obtained (the collector-emitter voltage $U_e = 350$ V).

Acknowledgments
The study was supported by a grant of the Russian Science Foundation (project No. 14-29-00231).

References
[1] Smirnov V P, Samokhin A A, Vorona N A and Gavrikov A V 2013 *Plasma Phys. Rep.* **39**(6) 456
[2] Litvak A, Agnew S, Anderegg F *et al.* 2003 *30th EPS Conference on Contr. Fusion and Plasma Phys.* vol 27A (St. Petersburg: Europhysics Conference Abstracts)
[3] Yuferov V B, Egorov A M, Ilichova V O, Shariy S V and Zhivankov K I 2013 *Problems of Atomic Science and Technology (PAST)* **84**(2) 148–151
[4] Papernyi V L and Lebedev N V 2014 *Plasma Phys. Rep.* **40**(1) 78–82
[5] Zhiltsov V A *et al.* 2006 *Atomic Energy* **101**(4) 755–759
[6] Amirov R *et al.* 2014 *J. Phys.: Conf. Series* **550**(1)
[7] Pavlov S L and Slotskii G L 1970 *JETP* **31**(1) 61–64
[8] Duman E L *et al.* 1982 Charge exchange processes (*Preprint* 3532/12)
[9] Freeman J H 1963 *Nucl. Instr. Meth.* **22** 306–316